



Original contribution

Expression pattern of androgen receptor and AR-V7 in androgen-deprivation therapy-naïve salivary duct carcinomas^{☆,☆☆}



Richard K. Yang MD, PhD^{a,1}, Pei Zhao PhD^{b,1}, Changxue Lu PhD^b, Jun Luo PhD^b, Rong Hu MD, PhD^{a,*}

^aDepartment of Pathology and Laboratory Medicine, University of Wisconsin, Madison, WI 53792, USA

^bDepartment of Urology, James Buchanan Brady Urological Institute, Johns Hopkins University, Baltimore, MD 21287, USA

Received 22 July 2018; revised 18 September 2018; accepted 19 September 2018

Keywords:

Salivary duct carcinoma;
Androgen-deprivation therapy;
Androgen receptor;
AR-V7;
RNA in situ hybridization;
Immunohistochemistry

Summary Androgen-deprivation therapy has been used to treat salivary duct carcinoma (SDC). The androgen receptor splice variant-7 (AR-V7) has been detected in castration-resistant prostate cancer and implicated in resistance to androgen receptor (AR)-targeted therapies. Given the potential role of AR/AR-V7 in SDC treatment, this study focuses on AR/AR-V7 expression in SDC specimens collected before androgen-deprivation therapy. RNA in situ hybridization (ISH) and immunohistochemistry (IHC) to detect total AR and AR-V7 were performed on formalin-fixed, paraffin-embedded SDC specimens from 23 patients. Full-length AR and AR-V7 transcripts were quantified in a subset of tumors by reverse-transcription polymerase chain reaction. Twenty SDCs were positive for total AR by ISH and IHC. Among AR-positive SDCs, 70% (14/20) were positive for AR-V7 messenger RNA by ISH, whereas 15% (3/20) were positive for AR-V7 protein by IHC. The 3 SDCs that expressed the highest levels of AR-V7 were all from female patients; one of them expressed a significant amount of AR-V7 and barely detectable full-length AR transcripts by reverse-transcription polymerase chain reaction. IHC expression of Forkhead box protein A1, prostate-specific antigen, prostatic acid phosphatase, and NKX3.1 was observed in some SDCs regardless of patient sex. Five SDCs demonstrated strong human epidermal growth factor receptor 2 expression. We conclude that treatment-naïve SDCs may express AR-V7 at levels comparable to or even exceeding the levels detected in castration-resistant prostate cancer. Our data support the feasibility to incorporate AR-V7 assessment via ISH and/or IHC in the ongoing clinical trials evaluating the therapeutic benefit of AR-targeted therapies in SDC patients.

© 2018 Elsevier Inc. All rights reserved.

[☆] Competing interest: The authors declare no conflict of interest.

^{☆☆} Funding/Support: This study was supported by research and development funding from the Department of Pathology and Laboratory Medicine, University of Wisconsin.

* Corresponding author at: Department of Pathology and Laboratory Medicine, University of Wisconsin, Madison, WI 53792.

E-mail address: rhu@uwhealth.org (R. Hu).

¹ These 2 authors contributed equally.

1. Introduction

Salivary duct carcinoma (SDC) is a rare and aggressive salivary gland malignancy often presenting with locally advanced disease or distant metastasis. Standard treatment of SDC is surgical resection with or without radiation therapy. The tumor is resistant to chemotherapy, and the mortality rate is high. Currently, there are only a few treatment modalities available for recurrent and metastatic SDC [1]. Amplification of human epidermal growth factor receptor 2 (HER2) has been detected in 15% to 50% of SDC. Trastuzumab, a HER2 inhibitor, has been tested with some clinical benefit in SDC patients [1,2]. However, controlled studies have not been done partly because of the rarity of this disease.

Normal salivary gland tissue expresses very little androgen receptor (AR) and is largely negative for AR by immunohistochemistry (IHC) staining. However, IHC staining of AR is positive in SDC, with a reported positivity rate ranging from 67% to 83%. In fact, a recent study has demonstrated up to 98% AR positivity by IHC in SDCs [3]. Androgen-deprivation therapy (ADT), a mainstay treatment of metastatic prostate cancer, has been used in the treatment of metastatic and recurrent AR-positive SDC. Case series have reported clinical benefit of ADT for patients with recurrent and/or metastatic AR-positive salivary gland cancer; most of these were patients with SDC or adenocarcinoma not otherwise specified [4-6]. Given the resistance of SDC to chemotherapy, as well as the emergence of AR as a promising treatment target, ADT has been considered a potential first-line systemic treatment for SDC patients. Clinical trials (NCT02749903, NCT01969578, and NCT02867852) are currently ongoing to investigate the efficacy of ADT in the treatment for male and female patients with recurrent or metastatic AR-positive salivary gland cancers [7]. These trials will shed light on the clinical benefits and limitations of ADT in AR-positive salivary gland cancers, most of which are SDCs. Among the questions to be interrogated are whether AR expression may be a clinically useful indication for ADT in SDC patients and how to select SDC patients who will benefit the most from ADT.

The mechanisms for castration resistance in prostate cancer have been studied extensively, and it has been generally accepted that despite castration levels of circulating androgen, AR signaling is sustained by bypassing the requirement for physiological levels of serum androgen in most castration-resistant prostate cancers (CRPCs). The mechanisms for sustained AR signaling under castration include the following: (1) adrenal and intratumoral androgen synthesis; (2) AR gene amplification resulting in elevated AR expression in tumor cells, which become supersensitive to castration levels of androgens; (3) AR gene mutations; and (4) constitutively active AR splice variants [8]. It remains largely unknown, however, whether similar mechanisms operate in SDC patients.

The AR gene consists of 8 canonical exons, of which exon 1 encodes the N-terminal domain, exons 2 and 3 encode the DNA binding domain (DBD), and exons 4 to 8 encode the

hinge region and the ligand binding domain. In comparison to the full-length AR (AR-FL), the splice variants retain the intact N-terminal domain and DBD but often do not have the ligand binding domain, mainly because of splicing of an intronic sequence to exons 1 to 3 (creating a cryptic exon) or exon skipping [9]. Among all AR splice variants identified so far, AR-V7 is the most abundant and most extensively characterized [8]. Although usually only expressed at a fraction of the levels of AR-FL, these splice variants are capable of maintaining AR signaling in the absence of ligands and therefore represent an important mechanism for castration resistance [10]. Several studies have shown that detection of AR-V7 messenger RNA (mRNA) or protein in circulating tumor cells from metastatic CRPC patients can be used as a biomarker to predict resistance to abiraterone or enzalutamide, 2 Food and Drug Administration–approved novel hormonal therapy agents for CRPC patients [11,12].

Despite the initial efficacy of ADT in SDC with an approximate 65% overall response rate, some patients have had disease recurrences subsequent to initial response, a scenario similar to those seen in CRPC. Furthermore, a small portion of AR-positive SDC patients do not respond to ADT therapy at all [5,6]. A study using frozen tissue has demonstrated the presence of AR splice variant AR-V7 mRNA in SDCs by reverse-transcription polymerase chain reaction (RT-PCR). This may represent an important molecular mechanism for resistance to ADT in SDC patients, similar to what is seen in prostate cancer [13]. A more recent study has shown the presence of AR-V7 in 8 of 16 SDC frozen specimens by RNA sequencing [14].

It is reasonable to hypothesize that AR-V7 may play important roles in the de novo or acquired ADT resistance developed initially or during disease recurrence subsequent to initial response to ADT in AR-positive SDC. Accordingly, SDC patients with AR-V7 overexpression may portend lack of benefit from ADT at treatment initiation. To investigate the mechanisms underlying the potential benefit of ADT and resistance to ADT in AR-positive SDC, this study aimed to interrogate AR and AR-V7 expression in SDC. We focused on establishing a clinically useful, reliable assay to detect AR-V7 in formalin-fixed, paraffin-embedded (FFPE) tissue and determining the frequency and pattern of AR and AR-V7 overexpression in SDC clinical specimens. By studying AR signaling using routine surgical pathology specimens, we sought to contribute to a strategic plan for the selection of SDC patients who may benefit the most from ADT.

2. Materials and methods

2.1. SDC tissue specimens

This study was performed in accordance with our institution's institutional review board approval. The Pathology Department electronic database for surgical pathology specimens

was searched for the diagnosis of “salivary duct carcinoma” between January 1, 2000, and January 1, 2017. Archived slides and FFPE blocks of available cases were retrieved. One FFPE block from each tumor was selected for studies.

2.2. Cell culture and cell block

Prostate cancer cell lines with known AR/AR-V7 status were used as controls, as described previously [15]. Briefly, PC3 cells were cultured in Dulbecco modified Eagle medium supplemented with 10% fetal bovine serum at 37°C in 5% CO₂. LNCaP95 cells of an androgen-independent cell line derived from parental LNCaP cell line were cultured in phenol red-free RPMI 1640 medium supplemented with 10% charcoal-stripped fetal bovine serum (CSS; Invitrogen, Carlsbad, CA). Cell pellets were fixed in 10% neutral-buffered formalin and embedded in paraffin.

2.3. Total AR and AR-V7 RNA in situ hybridization

RNA in situ hybridization (ISH) with probes targeting total AR and AR-V7 was performed using the RNAscope 2.5 HD Detection Reagent—RED (Advanced Cell Diagnostics, Hayward, CA). RNAscope Probe—Hs-AR-E1-E3 targeting AR exons 1 to 3 was used for total AR mRNA including AR-FL and AR splice variants. RNAscope Probe—Hs-AR-V*E targeting the cryptic exon 3 was used for AR-V7 mRNA detection (Fig. 1). Each probe consists of 18 to 20 pairs of oligonucleotides, which complementarily hybridize to their target sequences and span regions up to 1 kb long. ISH was performed as described previously [11]. LNCaP95 and PC-3 cell blocks were used as positive and negative controls, respectively, for the ISH. Briefly, freshly cut sections from FFPE clinical specimens or cell line blocks were baked at 60°C for

1 hour. The sections were then deparaffinized in xylene for 10 minutes before dehydration in 100% ethanol. The sections were air-dried and then hybridized with target probes at 40°C for 2 hours, followed by a series of preamplifier and amplifier steps. Slides were counterstained with 50% hematoxylin before signal detection.

2.4. Immunohistochemistry

IHC stains for total AR, HER2, prostate-specific antigen (PSA), prostate-specific acid phosphatase (PSAP), NKX3.1, and Forkhead box protein A1 (FOXA1) were performed on the Roche Ventana Medical System’s Discovery XT automated platform. All reagents were Roche-Ventana (Tucson, AZ) proprietary reagents except for the primary antibody diluent (Biocare Medical, Pacheco, CA) and Harris modified hematoxylin (ThermoFisher, Waltham, MA). The following primary antibodies were used: total AR (AR441; Dako, Carpinteria, CA), HER2 (SP3; ThermoFisher Scientific), PSA (ER-PR8; Cell Marque, Rocklin, CA), PSAP (PASE/4LJ; ThermoFisher), NKX3.1 (EP356; Cell Marque), and FOXA1 (ab5089 polyclonal IgG; Abcam, Cambridge, United Kingdom). Deparaffinization was carried out on the instrument, as was heat-induced epitope retrieval in the form of “cell conditioning” with CC1 (Tris-based, pH 8.5 for PSA, PSAP, NKX3.1, FOXA1) or with CC2 (citrate-based, pH 6.0 for HER2) for a duration of 44 minutes (HER2, FOXA1) or 28 minutes (PSA, PSAP, NKX3.1) at 95°C to 100°C. For primary antibody incubation, 100 µL of 1:50 (total AR), undiluted (PSA), 1:100 (HER2), 1:200 (NKX3.1, FOXA1), or 1:1500 (PSAP) antibody was diluted in DaVinci Green (PBS-based, pH 6.0; Biocare Medical; HER2, PSAP, NKX3.1) or Renoir Red (Tris-based, pH 6.2; Biocare Medical; FOXA1) diluent and was applied to tissue for 16 minutes (PSA), 28 minutes (PSAP, NKX3.1), or 60 minutes (HER2, FOXA1) at 37°C. After rinsing, Discovery OmniMap antirabbit (HER2, NKX3.1), antimouse (PSA, PSAP), or antigoat (FOXA1) horseradish peroxidase-conjugated secondary antibody was applied for 8 minutes at 37°C followed by rinsing. Discovery ChromoMap DAB detection kit (Ventana) was applied for a preset time, followed by rinsing and offline counterstaining with diluted Harris modified hematoxylin. Subsequent routine histology steps resulted in slides with permanent mounting media and No. 1.5 glass coverslips.

For IHC stain of AR-V7, deparaffinized FFPE sections underwent antigen retrieval in antigen unmasking solution, Tris-based high pH (H-3301; Vector Laboratories, Burlingame, CA), at 95°C for 20 minutes. The sections were incubated with monoclonal antihuman AR-V7 antibody (clone RM7, 1:200; RevMAb Biosciences, South San Francisco, CA) for 70 minutes at room temperature, rinsed, and then incubated with secondary antirabbit polyclonal IgG horseradish peroxidase (PowerVision, PV6118; Leica Biosystems, Buffalo Grove, IL) for 30 minutes at room temperature.

Full Length AR



AR-V7

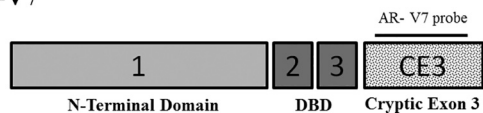


Fig. 1 Schematic illustration of exon compositions for the mRNA of AR-FL and AR-V7. Functional domains encoded by the exons as well as the ISH probe locations are marked. AR-V7 contains the intact N-terminal domain (encoded by exon 1) and DBD (encoded by exons 2/3) but lacks the ligand binding domain (encoded by exons 4/5/6/7/8). The total AR probe was designed to target exons 1 to 3 shared by AR-FL and AR splice variants. The AR-V7 probe was designed to target cryptic exon 3 (CE3) present in the AR-V7 mRNA but absent in the AR-FL mRNA.

Standardized 3,3'-diaminobenzidine and hematoxylin counterstains were used for signal development and detection.

2.5. Histologic scoring system

The ISH and IHC results were scored in a blinded semi-quantitative fashion by 2 pathologists (authors R. H. and R. Y.). ISH was scored 0 to 3+: a score of 3+ was given to signal that could be readily visualized at $\times 40$ magnification ($\times 4$ objective, $\times 10$ ocular); 2+ was signal that could be seen at $\times 100$; and 1+ was signal that was only seen at $\times 400$. For IHC stain, a semiquantitative score determined by the percentage of positively stained cells and the intensity of the stain between negative and 3+ was recorded holistically in a blinded fashion for nuclear stain (total AR, AR-V7, NKX3.1, and FOXA1) and cytoplasmic stain (PSA and PSAP) in the following manner: negative, no staining; 1+, less than 25% cells with weak staining; 2+, 25% to 75% cells with moderate

intensity; 3+, more than 75% cells with strong intensity. For HER2 staining, a score of 3+ was given to strong circumferential membranous staining of tumor cells, 2+ staining was weakly circumferential, and 1+ staining was partially membranous and noncircumferential staining. Contingency tables, Fisher exact tests, and χ^2 analysis testing were performed on GraphPad Prism version 7.02 (GraphPad Software, La Jolla, CA).

2.6. Reverse-transcription polymerase chain reaction

RT-PCR was performed to quantify the AR-FL and AR-V7 transcripts, respectively, as described previously [11]. Total RNA was extracted from FFPE sections (with target lesions marked by R. H.), followed by cDNA synthesis, creating template for quantitative RT-PCR. The RT-PCR primer sequences and reaction conditions used were described previously [11].

Patient subtypes	No.	%	Median OS after CT (mo)	<i>P</i>	Median OS after surgery (mo)	<i>P</i>
Overall	23	100	28.0		27.1	
Sex				.658 ^a		.759 ^a
Male	13	56.5	28.0		27.1	
Female	10	43.5	45.8		44.4	
Age (y)				.0009 ^a		.0017 ^a
<50	4	17.4	28.0		27.1	
50-70	13	56.5	61.4		56.8	
>70	6	26.1	11.5		9.4	
Clinical stage				.0010 ^b		.0019 ^b
I-III	7	30.4	NR		NR	
IVa	12	52.2	28.0		27.1	
IVc	4	17.4	9.7		9.3	
XRT or chemotherapy				.963 ^a		.735 ^a
Yes	16	69.6	28.0		27.1	
No	7	30.4	57.3		56.8	
Tumor size (cm)				.0187 ^b		.0424 ^b
0.0-2.0	9	39.1	NR		NR	
2.01-4.0	10	43.4	25.5		24.2	
>4.0	4	17.4	16.25		12.2	
Primary site				.988 ^a		.921 ^a
Parotid	21	91.3	28.0		27.1	
Submandibular	2	8.7	30.25		19.2	
Ex-PA				.849 ^a		.938 ^a
Yes	4	17.4	19.5		18.45	
No	19	82.6	36.9		27.1	
EtOH abuse Hx				.371 ^a		.691 ^a
Yes	8	34.8	25.5		24.2	
No	15	65.2	45.8		44.4	
Smoking Hx				.452 ^a		.435 ^a
Yes	14	61.9	57.3		44.4	
No	9	39.1	23.1		22.0	

Abbreviations: EtOH, Ethanol; Ex-PA, carcinoma ex-pleomorphic adenoma; NR, not yet reached median overall survival; XRT, radiation; OS, overall survival; CT, computed tomography; mo, month.

^a Denotes *P* value using log-rank testing.

^b Denotes *P* value for trend.

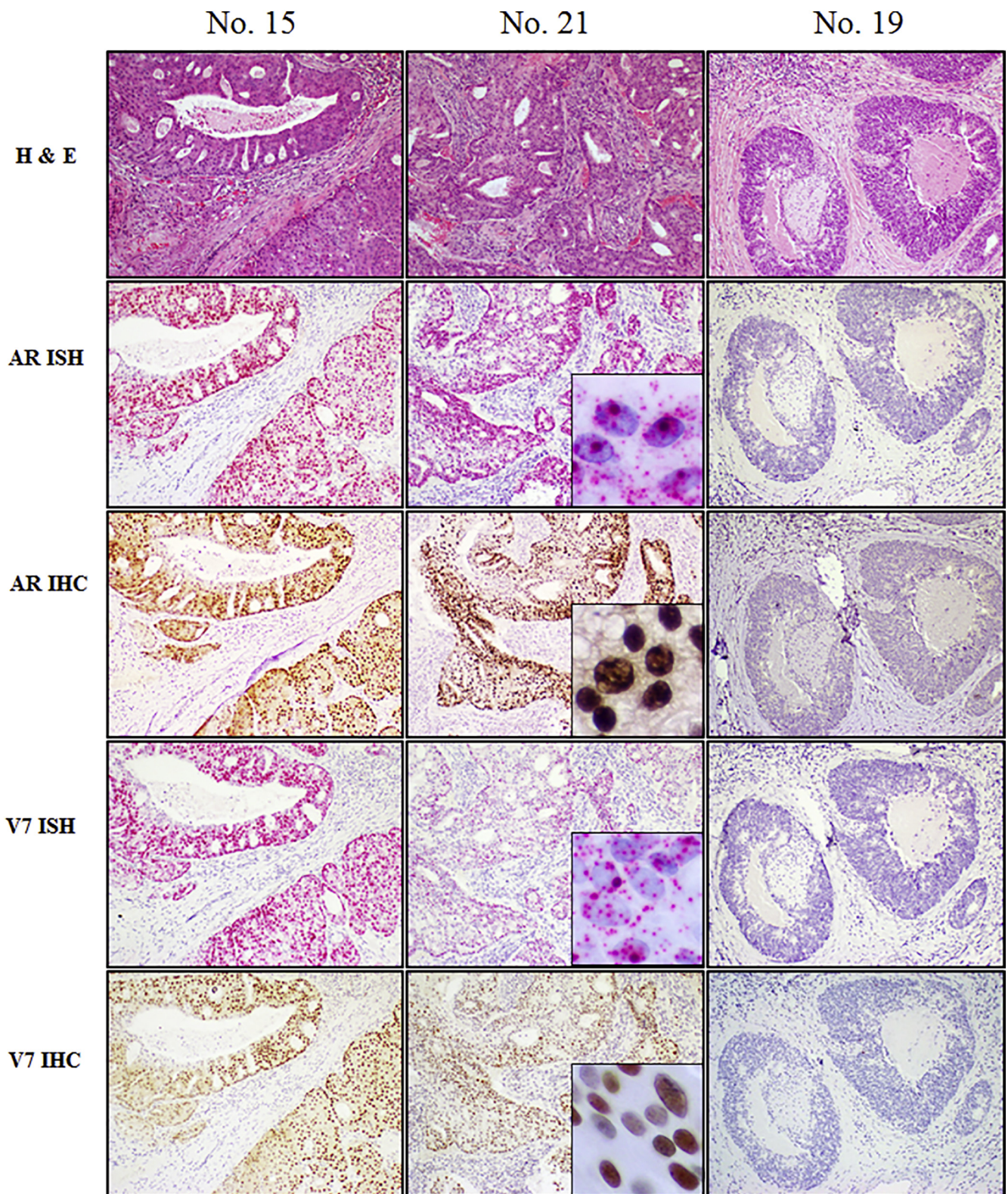


Fig. 2 Representative images from 3 SDC cases with various levels of total AR and AR-V7. Total AR was detected by AR ISH (mRNA) and AR IHC (protein), whereas AR-V7 was detected by V7 ISH (mRNA) and V7 IHC (protein). The specimen identification number is indicated on the top. Case 19 is negative for AR and AR-V7. Original magnification $\times 100$; inset magnification $\times 600$.

2.7. Survival analysis

Overall survival time in months was defined as the date of initial diagnostic computed tomography (CT) scan or date of surgical resection to the date of death or the date of last clinical evaluation if no death was documented. Survival (Kaplan-Meier) curves were created, and Mantel-Cox log rank analysis testing was performed on Prism version 7.02 (GraphPad). Because of the exploratory nature of these analyses, no corrections for multiple comparisons were made.

3. Results

3.1. SDC patient characteristics

The University of Wisconsin Health and Clinics Pathology archives were queried for histologically confirmed SDCs between January 1, 2000, and January 1, 2017. FFPE specimens from 23 SDC patients (13 men, 10 women) were retrieved. Patient ages ranged from 31 to 88 years, with a mean (SD) of 61 (14.5) years. Tumor sizes ranged from 0.8 to 10.0 cm, with a mean (SD) of 3.12 (2.2) cm. Sixteen (70%) of 23 patients were staged between stages IVa to IVc (American Joint Committee on Cancer), having at least moderately advanced local disease (pT4a), any nodal disease with a tumor size of greater than 3

cm (pN2), or metastatic disease (cM1). Three (13%) patients were staged between stages I to II, with tumors of 4 cm or less (pT1 or pT2) without nodal or distant metastatic disease. Four tumors (17%) were carcinoma ex-pleomorphic adenoma, 1 was minimally invasive and 3 were widely invasive. All patients underwent surgical resection of the tumor. Sixteen patients (70%) received adjuvant radiation therapy, 2 of whom also received adjuvant chemotherapy (Table), and none received ADT. Median overall survival was 27.1 months after surgery and 28 months after diagnostic CT scan. Both parameters demonstrated statistically significant associations with clinicopathological stage (Supplementary Fig. S1).

3.2. Total AR and AR-V7 expression in SDC clinical specimens

The LNCaP95 and PC-3 cell lines served as positive and negative controls for the ISH testing, respectively. ISH analysis demonstrated positive (3+) signal for both total AR and AR-V7 in LNCaP95 cells and was negative for both in PC-3 cells (data not shown). Twenty (87%) of 23 SDCs, 7 from female patients, were positive for total AR mRNA expression as demonstrated by the probe targeting total AR (Figs. 1 and 2, Supplementary Table S1). Most of the AR ISH-positive cases scored 2+ or 3+ (Fig. 2, Supplementary Table S1) in cancer tissue, whereas the

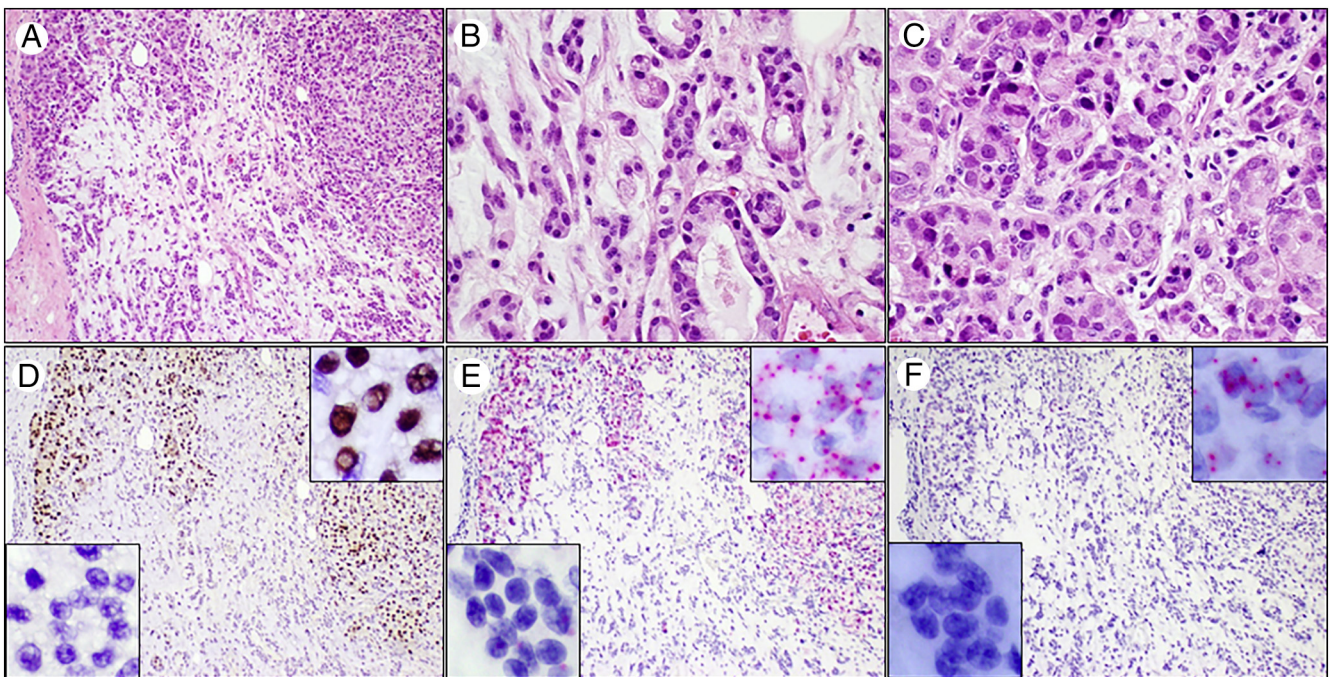


Fig. 3 Cancer-specific expression of ARs in a SDC ex pleomorphic adenoma. A, A relatively sharp demarcation between the benign-appearing pleomorphic adenoma (lower half of the image) and the SDC component (left and right upper corners) in a SDC ex-pleomorphic adenoma (original magnification $\times 100$). B, Higher magnification ($\times 400$) of the pleomorphic adenoma. C, Higher magnification ($\times 400$) of the SDC component. D, Distinct overexpression of AR proteins in the carcinomatous component but not in the cells in the maternal pleomorphic adenoma by AR IHC ($\times 100$). E and F, Distinct overexpression of total AR (E) and AR-V7 (F) mRNA in the carcinomatous component but not in the cells in the maternal pleomorphic adenoma by ISH. Left lower corner insets in panels D to F are amplified images ($\times 600$) from the benign-appearing pleomorphic adenoma. Right upper corner insets in panels D to F are amplified images ($\times 600$) from the carcinomatous component.

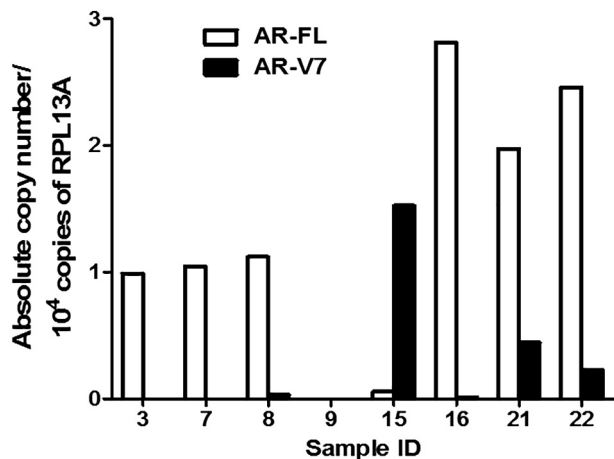


Fig. 4 Quantitation of AR-FL and AR-V7 mRNA by RT-PCR in eight SDCs. The *x*-axis represents specimen identification numbers. The *y*-axis measures the transcript copy numbers of AR-FL (white) and AR-V7 (black) mRNA transcripts per 10⁴ copies of RPL13A (a housekeeping gene used for data normalization) transcripts.

adjacent benign salivary gland tissue was AR ISH negative. The total AR mRNA expression was corroborated by protein expression demonstrated by IHC detecting all AR forms with an antibody targeting the N-terminal domain (Figs. 1 and 2, Supplementary Table S1). Notably, the total AR mRNA and protein binary (positive/negative) expression statuses demonstrated a 100% concordance. Three cases of AR-positive

SDCs were carcinoma ex-pleomorphic adenoma. One particular tumor (no. 12) showed a relatively sharp demarcation between the concurrent benign appearing pleomorphic adenoma and SDC (Fig. 3A-C) and was used to demonstrate cancer cell-specific expression of AR. As shown in Fig. 3D and E, the total AR mRNA and proteins were overexpressed in the carcinomatous component but largely negative in the benign-appearing pleomorphic adenoma component.

Fourteen (70%) of 20 AR-positive SDCs, 5 of which were from female patients, expressed AR-V7 mRNA detected by ISH. Expression signals in the 14 ISH-positive cases were generally lower in comparison to total AR, with the majority (*n* = 9) scoring 1+ (Fig. 3, Supplementary Table S1). Five tumors (nos. 15, 16, 21, 22, and 24), 4 of which were from female patients, expressed high AR-V7 mRNA (scores 2+ to 3+, ISH-high) at levels comparable to CRPC (Fig. 2, Supplementary Table S1). When stratified by sex, there seemed to be a statistically nonsignificant trend toward female patients expressing higher levels of AR-V7 mRNA by ISH (χ^2 test, *P* = .0625). Similar to total AR, AR-V7 mRNA was expressed in the carcinomatous component in case 12, but not in the benign-appearing pleomorphic adenoma component (Fig. 3F).

AR-V7 protein expression was detectable by IHC in 3 of 5 AR-V7 ISH-high SDCs (nos. 15, 21, and 24), but was not seen in the ISH-negative or ISH-low cases (Fig. 2, Supplementary Table S1). The AR-V7 protein expression was particularly strong in nos. 15 and 21 (Fig. 2). Interestingly, all 3 patients were women (Supplementary Table S1). A Fisher exact test

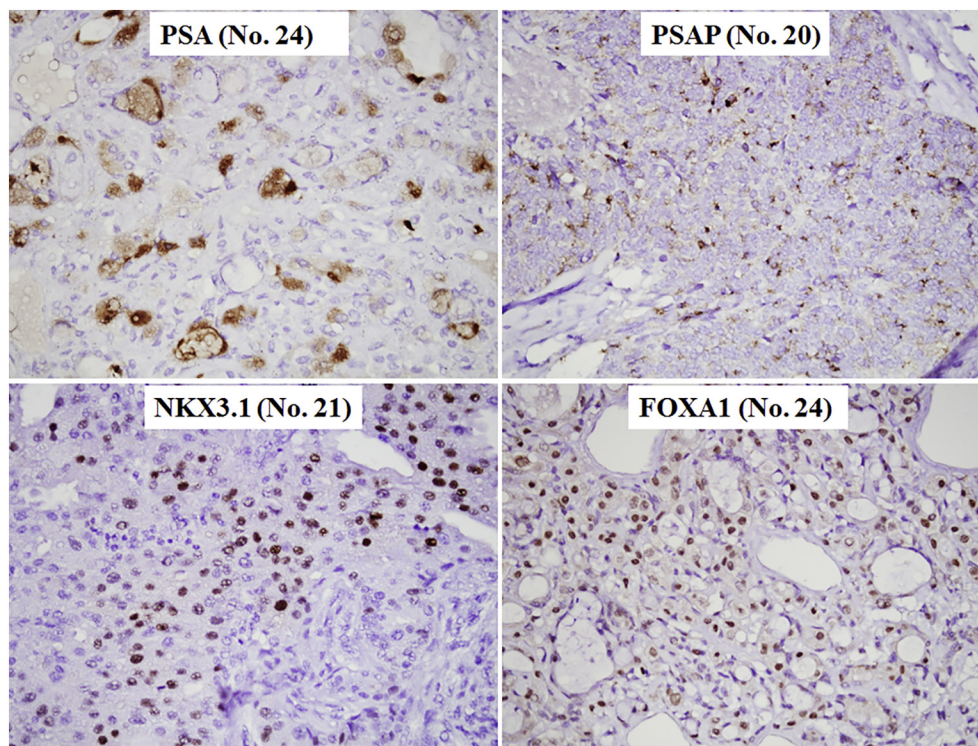


Fig. 5 Representative images of PSA, PSAP, NKX3.1, and FOXA1 IHC expression in SDCs. The panels portray cytoplasmic staining of PSA and PSAP and nuclear staining of NKX3.1 and FOXA1, respectively (original magnification $\times 400$). The specimen identification number is indicated in parenthesis.

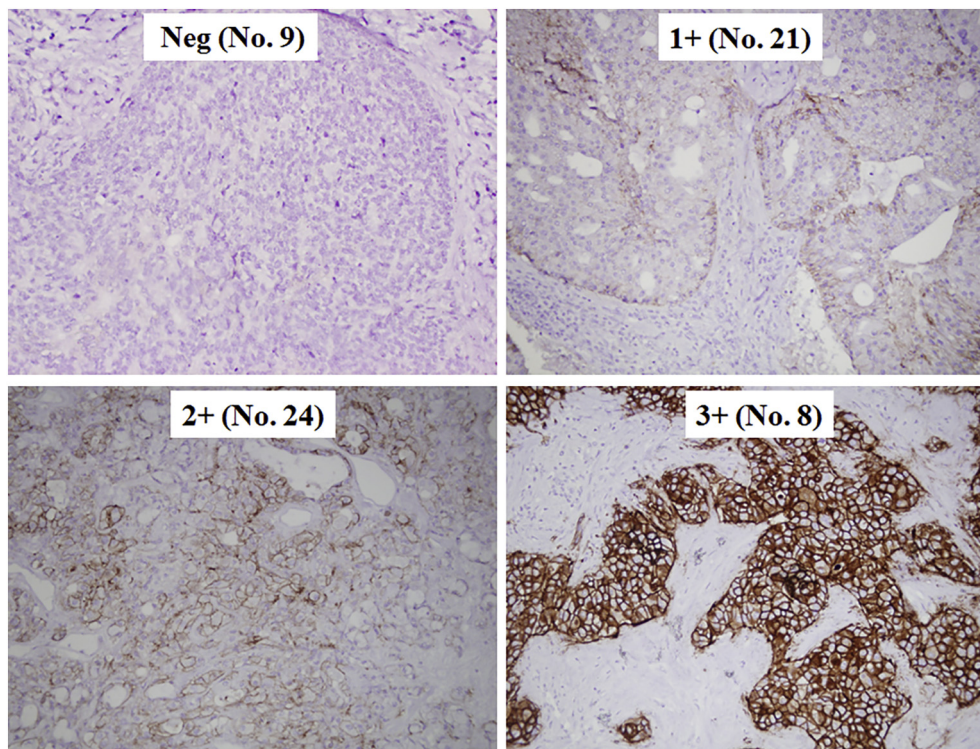


Fig. 6 Representative images of HER2 IHC in SDCs scored as negative (Neg), 1+, 2+, and 3+ based on the membranous staining (original magnification $\times 400$). The specimen identification number is indicated in parenthesis.

demonstrated a trend toward statistical significance ($P = .0596$) for this association.

3.3. Confirmation of AR-V7 mRNA overexpression in SDCs by RT-PCR

Eight SDCs were selected for quantitative RT-PCR analysis using primers specific for AR-FL and AR-V7, respectively. AR-FL was positive by RT-PCR in 6 SDC tumors, all of which were positive for total AR by ISH and IHC analyses (Fig. 4, Supplementary Table S1). Three tumors (nos. 15, 21, and 22) were positive for AR-V7 mRNA by RT-PCR. Notably, case 15 demonstrated an unusual pattern of AR expression, showing extremely high AR-V7 expression, whereas AR-FL mRNA was barely detectable by RT-PCR (Fig. 4). Case 15 also demonstrated the highest AR-V7 expression by both ISH and IHC (Fig. 2, Supplementary Table S1). Therefore, the signals of total AR demonstrated by the ISH and IHC analyses were mostly attributed to AR-V7 in this case. Case 9 was RT-PCR negative for AR-FL/AR-V7 transcripts, a finding consistent with AR/AR-V7 ISH.

3.4. Expression of PSA, PSAP, NKX3.1, and FOXA1 in SDCs

Expression of prostate markers PSA (2 cases; 9%), PSAP (7 cases; 30%), and NKX3.1 (3 cases; 12%) was detected in SDCs by IHC (Supplementary Table S1). Positive staining was often

focal rather than diffuse. Expression of these markers was not seen in adjacent benign salivary gland tissue. Fourteen SDCs (61%) demonstrated low (1+) to moderate (2+) FOXA1 expression by IHC (Supplementary Table S1) in tumor tissue. Expression of FOXA1 was not observed in the adjacent benign salivary gland tissue. Moderate expression of PSAP was seen in one AR-negative SDC (no. 9), whereas none of the AR-negative SDC expressed PSA, NKX3.1, or FOXA1 (Supplementary Table S1). Representative IHC images of PSA, PSAP, NKX3.1, and FOXA1 are shown in Fig. 5.

3.5. HER2 overexpression in SDCs

Sixteen (70%) of 23 SDCs demonstrated some amount of membranous HER2 expression by IHC. Five tumors (22%) showed strong (3+) HER2 expression, whereas HER2 expression was weaker in 11 SDCs (48%) (Supplementary Table S1). The HER2 expression levels in the male and female patients were similar. Expression of HER2 and AR-V7 was not mutually exclusive. However, SDCs with the highest HER2 expression (3+) were either negative or low for AR-V7 expression by ISH. Representative images of HER2 membranous stain are shown in Fig. 6.

4. Discussion

SDC is a rare high-grade salivary gland malignancy. Surgical resection with or without adjuvant radiation is the primary

treatment modality. The abysmal prognosis of this disease was redemonstrated by the follow-up data that we retrieved from this single-institution cohort. Several clinical trials are underway investigating ADT as a systemic treatment of SDC, given that AR is overexpressed in most SDCs but not in benign salivary gland tissue. Small case series have shown that some SDCs do not respond to ADT at all, and some SDCs recur under castration despite an initial response to ADT, a situation similar to those seen in CRPC, a more common but still lethal malignancy. During the past few decades, extensive studies on mechanisms of CRPC have led to the development of strategies to treat CRPC and to select patients who will benefit from AR-targeted therapies. AR-V7 has been found to play an important role in the development of CRPC and has been explored as a biomarker to predict diminished or lack of response to AR-targeted therapies in prostate cancer patients [8,10,11].

A few previous studies have demonstrated the presence of AR-V7 mRNA in SDC frozen tissue [13,14]. This study sought to develop and validate assays that can be applied to surgical pathology specimens in the clinical setting by ISH and IHC. Our data have shown that ISH was a sensitive and highly specific method to detect both total AR and AR-V7 in FFPE specimens, and that this test could be done routinely using commercially available reagents. AR-V7 IHC staining was less sensitive but highly specific in detecting AR-V7 protein expressed at levels that may be more clinically relevant. The specificity of AR-V7 detection was confirmed by quantitative RT-PCR. To the best of our knowledge, this is the first report demonstrating AR-V7 protein expression in SDCs.

Unlike in prostate cancer, in which AR-V7 is usually overexpressed after ADT, we found validated AR-V7 expression in SDC patients without prior exposure to ADT. There seemed to be a nonsignificant trend toward female patients expressing higher levels of AR-V7 mRNA by ISH. In addition, all 3 AR-V7 protein-positive SDC patients were women. Unexpectedly, 2 tumors expressed AR-V7 protein at levels comparable to or even exceeding the levels detected in CRPC. It is reasonable to speculate that tumor cells overexpressing AR-V7, a constitutively active variant in the absence of ligands, may have a growth advantage over tumors only expressing AR-FL, which requires androgen for functioning, in the female patients in whom androgen levels are low and comparable to those in castrated male patients. We anticipate that patients with high levels of AR-V7 expression would be less likely to benefit from ADT based on analogous data from prostate cancer studies [11,15]. This hypothesis needs to be tested in large cohorts of SDC patients treated with AR-targeted therapies (none of the patients in our cohort received ADT). Therefore, it is important to incorporate testing of AR-V7 in SDCs at various stages (before and after treatment) during the ongoing multi-institutional clinical trials using ADT in treatment regimens to determine whether AR-V7 can serve as a prognostic or predictive biomarker for hormonal therapy response. Based on our findings, the testing can be done conveniently by standard ISH and/or IHC using commercially available reagents if

validated by independent studies. Questions that need to be answered in these clinical trials may include the following: (1) Does SDC expressing high levels of AR-V7 respond to ADT at initiation? (2) Does AR-V7 expression increase during ADT treatment? and (3) If so, does the tumor lose the responsiveness to ADT as CRPC does?

The mechanisms underlying AR/AR-V7 overexpression in SDCs are still unclear. The role that AR singling may play in the development of SDC has not been well characterized. We observed total AR and AR-V7 overexpression in the SDC, but not in its concurrent maternal pleomorphic adenoma in a SDC ex-pleomorphic adenoma (Fig. 3). This finding needs validation from a larger cohort study and may suggest a role for AR in the pathogenesis of AR-positive SDCs.

FOXA1 is a key member of the AR transcriptional complex, and overexpression of FOXA1 has been noted in metastatic prostate cancers and CRPC [16]. Mutations within the DBD of FOXA1 have been reported in CRPC. Similarly, mutations of FOXA1 within the DBD have been described in SDCs [14]. Our IHC analysis showed some amount of FOXA1 expression in 61% of SDCs, all of which were positive for AR. Focal expression of prostate-specific markers PSA, PSAP, and NKX3.1 was found in a few AR-positive SDCs irrespective of patient sex, and moderate PSAP expression was observed in one AR-negative SDC. These findings are somewhat different from those observed in prostate cancer, suggesting potentially distinct and context-specific AR signaling pathways between prostate cancer and SDC. These data are relevant to pathology practice; IHC staining of prostate-specific markers should be interpreted with caution in appropriate morphologic context when determining whether a metastatic tumor is of prostate origin, especially when the patients have a history of salivary gland malignancy.

We found that 70% of SDCs expressed some amount of HER2 and that strong, robust expression (3+) by IHC was present in 5 tumors (22%), likely due to *HER2/neu* gene amplification. Although overexpression of HER2 and AR-V7 was not mutually exclusive, SDCs with the highest HER2 expression (3+) were either negative or low for AR-V7 expression (Supplementary Table 1), suggesting possible independent pathways in the oncogenesis of these SDCs.

To summarize, we have detected overexpression of AR-V7, a constitutively active splice variant of AR, at both transcript and protein levels in ADT-naïve SDCs. We hypothesize that this subset of patients may benefit less from ADT. This hypothesis needs to be tested by studying patients treated with ADT. Therefore, it is crucial to incorporate AR-V7 testing during the ongoing clinical trials giving ADT to SDC patients. Data retrieved from such studies will help build a strategic plan to select patients who may benefit the most from ADT in the future. The testing can be done conveniently on FFPE clinical specimens by standard RNA ISH and/or IHC without the need to obtain frozen tissue. Given the interesting results that we have obtained so far, we believe that further exploration on the mechanisms underlying AR-V7 overexpression in SDC is also warranted.

Supplementary data

Supplementary data to this article can be found online at <https://doi.org/10.1016/j.humpath.2018.09.009>.

Acknowledgments

The authors thank the University of Wisconsin Translational Research Initiatives in Pathology laboratory, in part supported by the UW Department of Pathology and Laboratory Medicine and UWCCC grant P30 CA014520, for use of its facilities and services.

References

- [1] Limaye SA, Posner MR, Krane JF, et al. Trastuzumab for the treatment of salivary duct carcinoma. *Oncologist* 2013;18:294-300.
- [2] Falchook GS, Moulder S, Naing A, et al. A phase I trial of combination trastuzumab, lapatinib, and bevacizumab in patients with advanced cancer. *Invest New Drugs* 2015;33:177-86.
- [3] Williams L, Thompson LD, Seethala RR, et al. Salivary duct carcinoma: the predominance of apocrine morphology, prevalence of histologic variants, and androgen receptor expression. *Am J Surg Pathol* 2015;39:705-13.
- [4] Locati LD, Perrone F, Cortelazzi B, et al. Activity of abiraterone in rechallenging two AR-expressing salivary gland adenocarcinomas, resistant to androgen-deprivation therapy. *Cancer Biol Ther* 2014;15:678-82.
- [5] Locati LD, Perrone F, Cortelazzi B, et al. Clinical activity of androgen-deprivation therapy in patients with metastatic/relapsed androgen receptor-positive salivary gland cancers. *Head Neck* 2016;38:724-31.
- [6] Yamamoto N, Minami S, Fujii M. Clinicopathologic study of salivary duct carcinoma and the efficacy of androgen-deprivation therapy. *Am J Otolaryngol* 2014;35:731-5.
- [7] Dalin MG, Watson PA, Ho AL, Morris LG. Androgen receptor signaling in salivary gland cancer. *Cancers (Basel)* 2017;9:17-26.
- [8] Lu C, Luo J. Decoding the androgen receptor splice variants. *Transl Androl Urol* 2013;2:178-86.
- [9] Hu R, Isaacs WB, Luo J. A snapshot of the expression signature of androgen receptor splicing variants and their distinctive transcriptional activities. *Prostate* 2011;71:1656-67.
- [10] Hu R, Dunn TA, Wei S, et al. Ligand-independent androgen receptor variants derived from splicing of cryptic exons signify hormone-refractory prostate cancer. *Cancer Res* 2009;69:16-22.
- [11] Antonarakis ES, Lu C, Wang H, et al. AR-V7 and resistance to enzalutamide and abiraterone in prostate cancer. *N Engl J Med* 2014;371:1028-38.
- [12] Scher HI, Lu D, Schreiber NA, et al. Association of AR-V7 on circulating tumor cells as a treatment-specific biomarker with outcomes and survival in castration-resistant prostate cancer. *JAMA Oncol* 2016;2:1441-9.
- [13] Mitani Y, Rao PH, Maity SN, et al. Alterations associated with androgen receptor gene activation in salivary duct carcinoma of both sexes: potential therapeutic ramifications. *Clin Cancer Res* 2014;20:6570-81.
- [14] Dalin MG, Desrichard A, Katabi N, et al. Comprehensive molecular characterization of salivary duct carcinoma reveals actionable targets and similarity to apocrine breast cancer. *Clin Cancer Res* 2016;20:4623-33.
- [15] Zhu Y, Sharp A, Anderson CM, et al. Novel junction-specific and quantifiable in situ detection of AR-V7 and its clinical correlates in metastatic castration-resistant prostate cancer. *Eur Urol* 2018;73:727-35.
- [16] Robinson JL, Hickey TE, Warren AY, et al. Elevated levels of FOXA1 facilitate androgen receptor chromatin binding resulting in a CRPC-like phenotype. *Oncogene* 2014;33:5666-74.